Electronic Supplementary Information

Wearable, fast healable, and self-adhesive multifunctional photoactive hydrogel for strain and temperature sensor

He Zhu [a],Jing Xu [a,b], Xin Sun [a,b], Qikai Guo [a], Qinglei Guo [a], Mingshun Jiang [c], Kejun Wu [d], Rong Cai,*[e] Kai Qian*[a,b]

[a] School of Microelectronics, Shandong University, Jinan, 250100, China

E-mail: kaiqian@sdu.edu.cn

[b] Shenzhen Research Institute of Shandong University, Shenzhen, 518057, China

[c] School of Control Science and Engineering, Shandong University, Jinan 250061, China

[d] State Key Lab of Electronic Thin Films and Integrated Devices, University of Electronic Science and Technology of China, Chengdu, 610054, China

[e] School of Pharmaceutical Sciences, Shandong University, Jinan, 250012, China

E-mail: rongcai@sdu.edu.cn

This File Includes:

Supplementary Figures S1 to S8

Supplementary Table S1 to S2

Supplementary Movies S1 to S2

Supplementary Figures

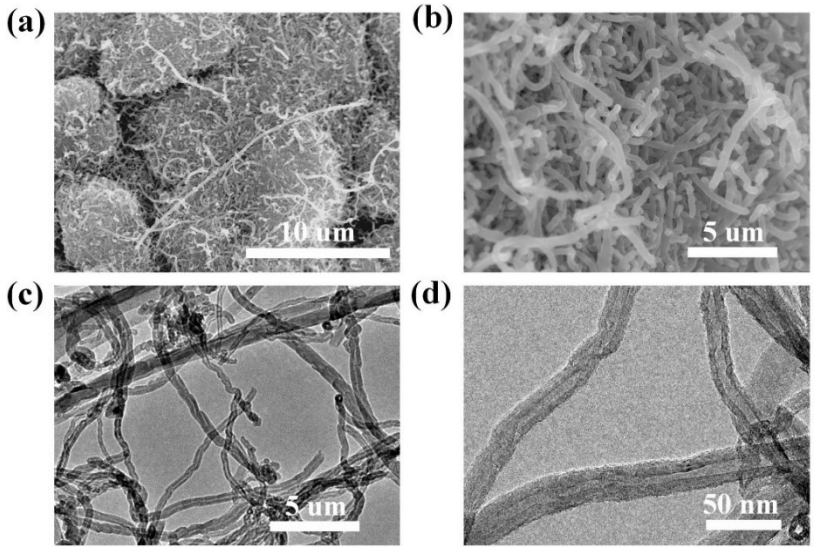

Fig. S1 (a, b) SEM and (c, d) TEM images of the morphology of CNTs modified by PDA.

The morphology of CNTs modified by PDA (d-CNTs) was characterized using SEM and TEM, respectively. As shown in **Fig S1a-d**, the d-CNTs exhibited tube-like shape with length of ~10-20μm and outside diameter of around 30-50 nm.

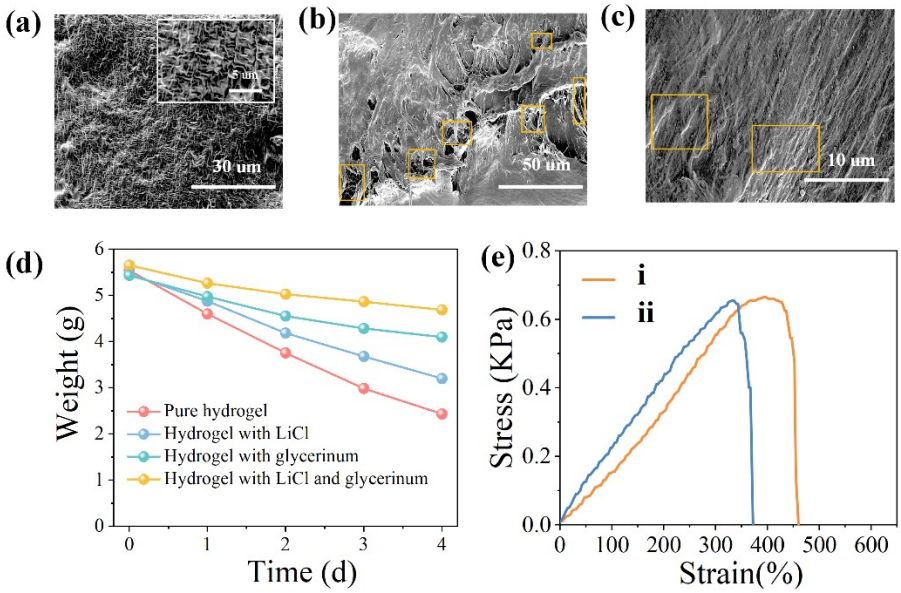

Fig. S2 (a) SEM image of the freeze-dried PVA/d-CNTs hydrogel with porous network structure. (b) SEM image of d-CNTs distribution inside the PVA hydrogel. (c) SEM image of d-CNTs distribution on the PVA hydrogel surface. (d) The weight loss of the PVA/d-CNTs

hydrogel before and after addition of glycerinum and LiCl. (e) Mechanical properties of PVA/d-CNTs hydrogel(i) and pure PVA hydrogel(ii).

As shown in **Fig. S2d**, compared to the pure hydrogel, the hydrogel containing LiCl lost weight more slowly. In addition, the water molecules in the hydrogel also can be partially replaced by organic agent of glycerinum, which form strong hydrogen bonds between the agent and the water molecules that compete with the original hydrogen bonds in water, [1] resulting in decreased drying speed of the resultant organohydrogels. Therefore, both LiCl and glycerinum were added in the hydrogel, which can greatly improve the water retention capacity of hydrogel. [2,3]

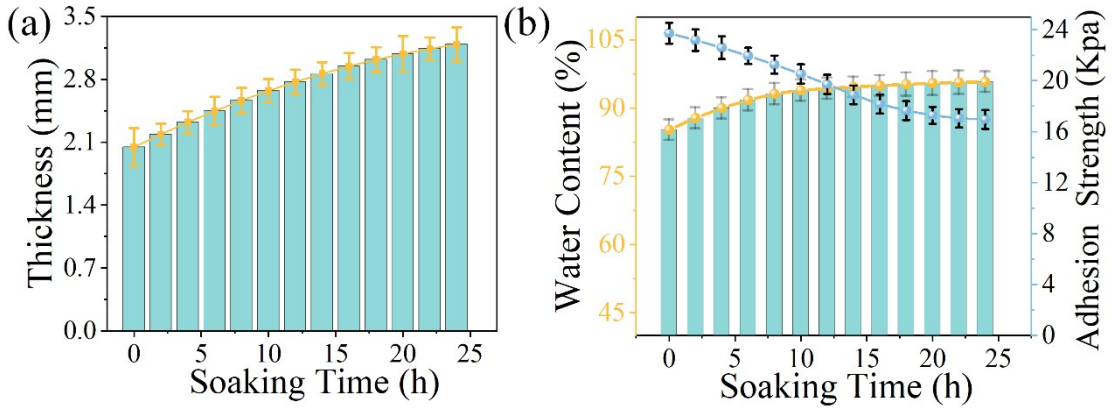

Fig. S3 (a) The relationship between PVA/d-CNTs hydrogel thickness and soaking time. (b) Variation of water content and adhesion on glass substrate with soaking time.

Generally, the hydrogels adhesion strength could be affected by the following factors [4]: (1) the surface chain density and bulk energy dissipation of the hydrogel; (2) the water content and effective contact area over the interface between the hydrogel and substrate. Specifically, the soaking time would change the hydrogel self-adhesive property by affecting the water content of hydrogel. [4-6] As shown in **Figure S3a**, the PVA/d-CNTs hydrogel thickness increased with soaking time, which provided more space for the polymer chain to expand. The water content in hydrogel also increased with soaking time, which resulted in the polymer network extension and surface chain density decrease, leading to the weakened adhesion strength on glass substrate **(Figure S3b)**.

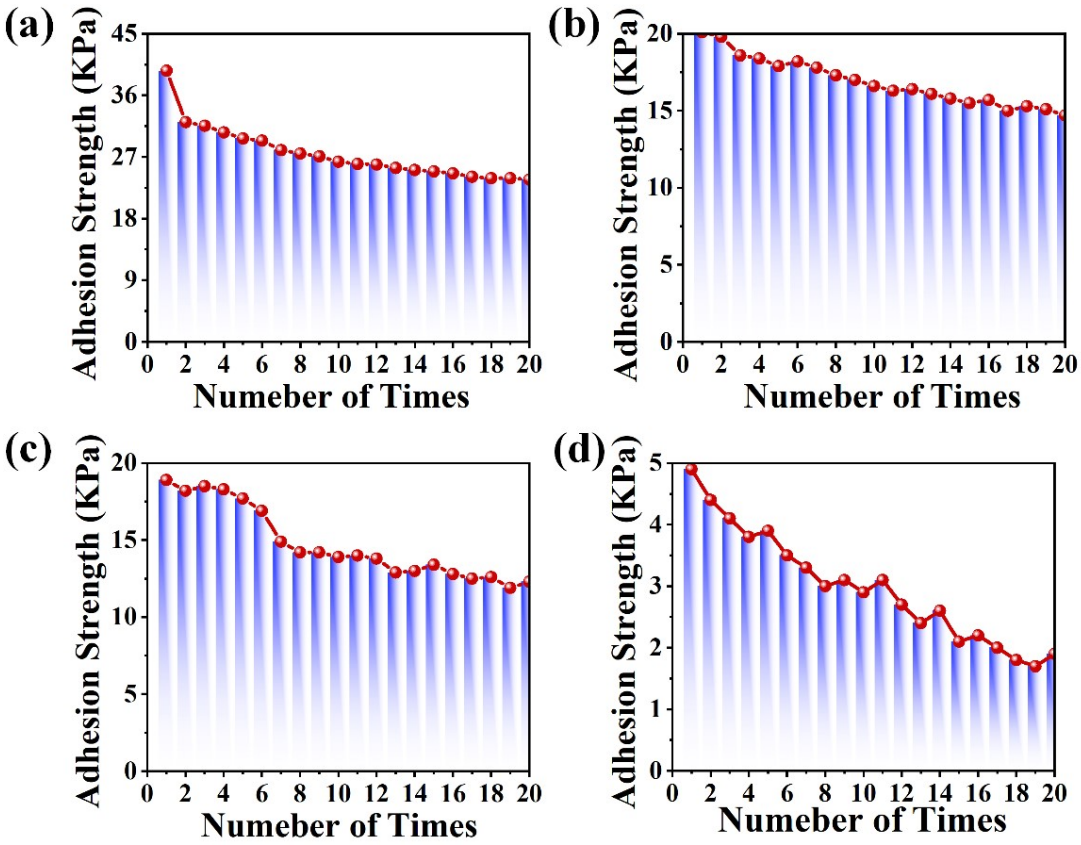

Fig. S4 Repeatable adhesion properties of PVA/CNTs to human latex gloves (a), plastic (b), glass (c) and metal (d).

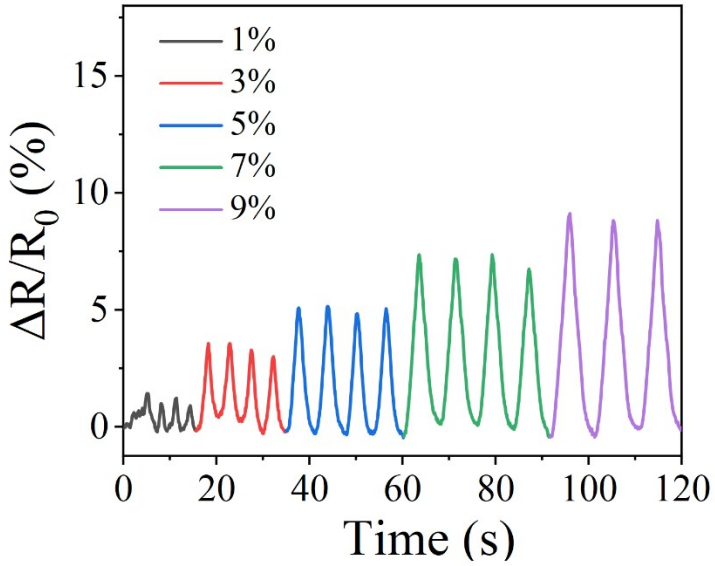

Fig. S5 Relative resistance changes ($\Delta R/R_0$) of PVA/d-CNTs hydrogel sensor upon four stretching-releasing cycles at strains less than 10%.

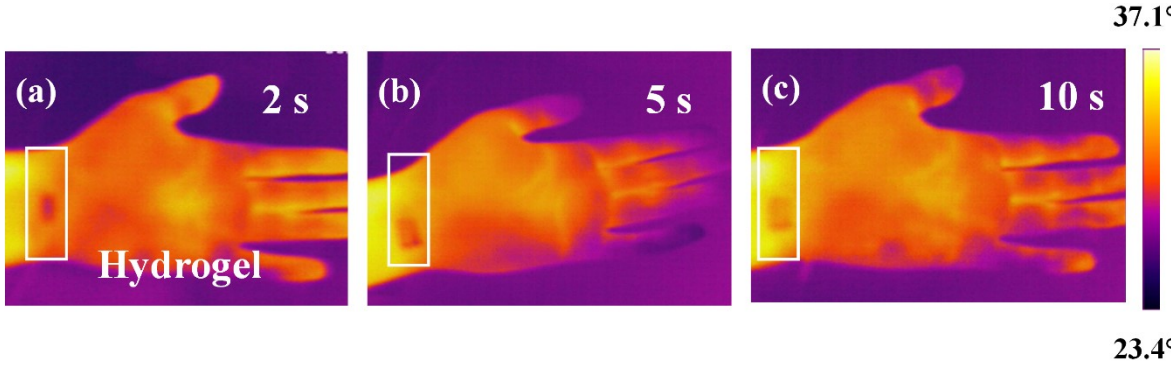

Fig. S6 PVA/d-CNTs hydrogel attached to the volunteers' skin was able to match the skin temperature for (a) 2 s, (b) 5 s and (c) 10 s at room temperature.

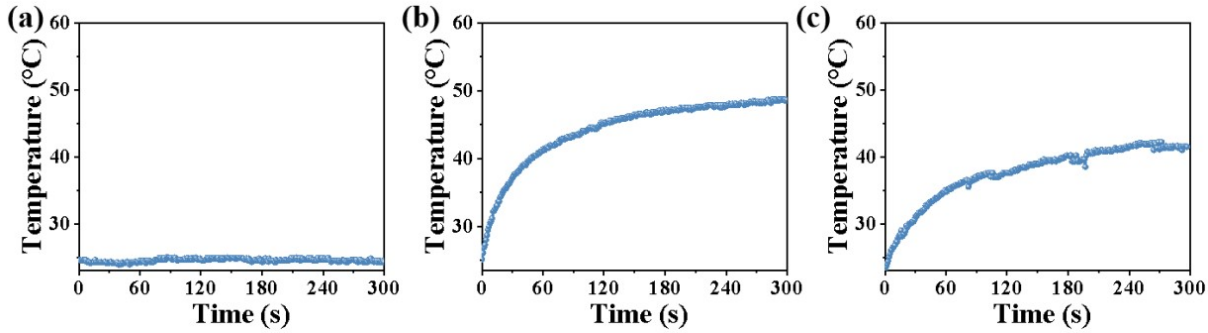

Fig. S7 Photothermal curves of (a) pure PVA and (b) PVA mixed with CNTs hydrogels and (c) PVA mixed with poly(dopamine) hydrogels under exposure to NIR laser (λ=980 nm) irradiation with power density of 200 mW/cm^2.

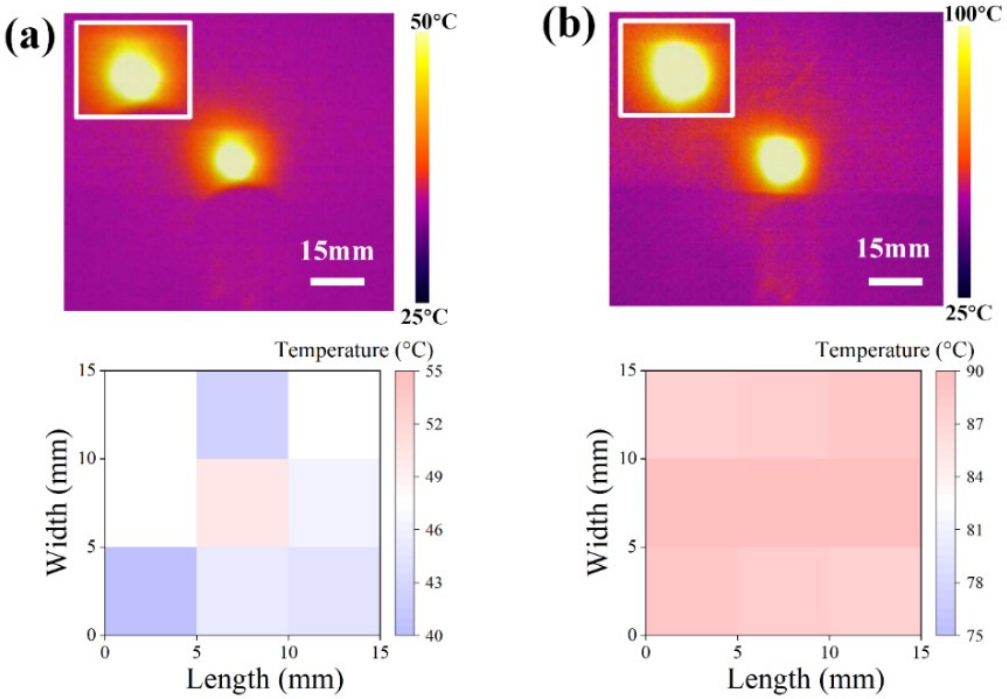

Fig. S8 Infrared images and temperature distribution of (a) PVA/CNTs hydrogel and (b) PVA/d-CNTs hydrogel under near-infrared laser irradiation with power density of 200 mW/cm^2.

Supplementary Table

Table S1. The self-healing performance comparisons for different hydrogels.

Ref	Materials	Healing condition	Healing efficiency
[7]	PVA/PIE	5 min	69.46%
[8]	PAA-CNF-LMNPs	3 h	65 %
[9]	PVI-ChCl-PDO	12 h	88.9%
[10]	nPHHs/ PANI-NPs	1 s	33.87%
[11]	PAAm	12 h	98.6%
[12]	PBA-IL	150 min	91.98%
[13]	PVA	12 h	72%
[14]	TOCNF	10 s	95%
[15]	Protein	1 s	95.8%
This work	PVA/d-CNTs	5 s	83.08%

Table S2. Temperature sensors performance comparison for different materials.

Ref	Materials	TCR(%/°C)	Self-healing	Test range(°C)
[16]	Ag NFs/Ag NWs	0.03	no	30-45
[17]	Ag nanocrystal/PDMS	0.185	no	30-50
[18]	CNT TFT	1.9	no	25-60
[19]	PANI NFs Hydrogel	1.64	yes	40-110
[20]	oligomers/SWCNTs	0.78	yes	0-80
[21]	MXene Hydrogel	5.27	no	0-80
This work	PVA/CNT Hydrogel	2.7	yes	25-75

Supplementary Movies

Supplementary Movie S1. The real-time monitoring for finger motion with a wireless system.

Supplementary Movie S2. Alarm circuit with a liquid crystal display for high temperature perception.

Reference

[1] Y. Wei, L. Xiang, H. Ou, F.Li, Y. Zhang, Y. Qian, L. Hao, J. Diao, M. Zhang, P. Zhu, Y. Liu, Y. Kuang and G. Chen, *Adv. Funct. Mater*., 2020, **30**, 2005135.

[2] Y. Niu, H. Liu, R. He, M. Luo, M. Shu and F. Xu, *Small*, 2021, **17**, 2101151.

[3] Q. Zhang, X. Hou, X. Liu, X. Xie, L. Duan, W. Lü and G. Gao, *Small*, 2021,**17**, 2103091.

[4] Z. Zhou, J. Lei and Z. Liu, *Polymer*, 2022, **246**, 124730.

[5] W. Kim, Y. Han, I. S. Lee, N. Won and Y. Na, *Polymer*, 2022, **255**, 125112.

[6] J. Zhang, Y. Wang, J. Zhang, I. M. Lei, G. Chen, Y. Xue, X. Liang, D. Wang, G. Wang, S. He and J. Liu, *Small*, 2022, **18**, 2201796.

[7] C. Wang, Y. Liu, X. Qu, B. Shi, Q. Zheng, X. Lin, S. Chao, C. Wang, J. Zhou, Y. Sun, G. Mao and Z. Li, *Adv. Mater.*, 2022, **34**, 202105416.

[8] Y. Ye and F. Jiang, *Nano Energy*, 2022, **99**, 107374.

[9] K. Fan, W. Wei, Z. Zhang, B. Liu, W. Feng, Y. Ma and X. Zhang, *Chem. Eng. J.*, 2022, **449**,137878.

[10] X. Yu, H. Zhang, Y. Wang, X. Fan, Z. Li, X. Zhang and T. Liu, *Adv. Funct. Mater.*, 2022, 2204366.

[11] X. Dai, L. Huang, Z. Sun, Y. Du, B. Xue, M. Wong, J. Han, Q. Liang, Y. Wu, B. Dong, J. Kong and J. Hao, *Mater. Horizons*, 2022, **9**, 1412–1421

[12] X. Yao, S. Zhang, L. Qian, N. Wei, V. Nica, S. Coseri and F. Han, *Adv. Funct. Mater.*, 2022, 2204565.

[13] M. Caprioli, I. Roppolo, A. Chiappone, L. Larush, C. F. Pirri and S. Magdassi, *Nat Commun.*, 2021, **12**, 2462.

[14] Y. Qin, J. Mo, Y. Liu, S. Zhang, J. Wang, Q. Fu, S. Wang and S. Nie, *Adv. Funct. Mater.*, 2022, 2201846.

[15] A. Pena-Francesch, H. Jung, M. Demirel and M. Sitti, *Nat. Mater.*, 2020, **19**, 1230-1235.

[16] B. W. An, S. Heo, S. Ji, F. Bien and J.U. Park, *Nat. Commun.*, 2018, **9**, 2458.

[17] J. Bang, W. S. Lee, B. Park, H. Joh, H. K. Woo, S. Jeon, J. Ahn, C. Jeong, T. i. Kim and S. J. Oh, *Adv. Funct. Mater.*, 2019, **29**, 1903047.

[18] C. Zhu, A. Chortos, Y. Wang, R. Pfattner, T. Lei, A. Hinckley, I. Pochorovski, X. Yan, J. To, J. Oh, J. Tok and Z. Bao, B. Murmann, *Nat. Electron.*, 2018, **1**, 183.

[19] G. Ge, Y. Lu, X. Qu, W. Zhao, Y. Ren, W. Wang, Q. Wang, W. Huang and X. Dong, *ACS Nano*, 2019, **14**, 218.

[20] H. Yang, D. Qi, Z. Liu, K. Chandran., T. Wang, J. Yu, and X. Chen, *Adv. Mater.*, 2016, **28**, 9175–9181.

[21] H. Liu, C. Du, L. Liao, H. Zhang, H. Zhou, T. Ren, Z. Sun, Y. Lu, Z. Nie, F. Xu, J. Zhu and W. Huang, *Nat. Commun.*, 2022, **13**, 3420.